Mineralogical Magazine, June 2015, Vol. 79(3), pp. 735–753

Ferriakasakaite-(La) and ferriandrosite-(La): new epidote-supergroup minerals from Ise, Mie Prefecture, Japan

Mariko Nagashima[1,*], Daisuke Nishio-Hamane[2], Norimitsu Tomita[3], Tetsuo Minakawa[3] and Sachio Inaba[4]

[1] Graduate School of Science and Engineering, Yamaguchi University, Yamaguchi 753-8512, Japan
[2] The Institute for Solid State Physics, the University of Tokyo, Kashiwa, Chiba 277-8581, Japan
[3] Department of Earth Science, Faculty of Science, Ehime University, Matsuyama, Ehime 790-8577, Japan
[4] Inaba-Shinju Corporation, Minami-ise, Mie 516-0109, Japan

[*Received 24 July 2014; Accepted 9 December 2014; Associate Editor: E. Grew*]

ABSTRACT

The new *REE*-rich, monoclinic, epidote-supergroup minerals ferriakasakaite-(La) and ferriandrosite-(La), found in tephroite ± calcite veinlets cutting the stratiform ferromanganese deposit from the Shobu area, Ise City, Mie Prefecture, Japan, were studied using electron microprobe analysis and single-crystal X-ray diffraction methods. Ferriakasakaite-(La), ideally $^{A1}Ca^{A2}La^{M1}Fe^{3+M2}Al^{M3}Mn^{2+}(SiO_4)(Si_2O_7)O(OH)$ (Z = 2, space group $P2_1/m$), has a new combination of dominant cations at $A1$(Ca) and $M3$(Mn^{2+}), which are the key sites to determine a root name for epidote-supergroup minerals. The unit-cell parameters are a = 8.8733(2), b = 5.7415(1), c = 10.0805(3) Å, β = 113.845(2)° and V = 469.73(2) Å^3. According to the structural refinement (R_1 = 3.13%), the determined structural formula is $^{A1}(Ca_{0.54}Mn^{2+}_{0.46})^{A2}[(La_{0.48}Ce_{0.20}Pr_{0.07}Nd_{0.18}Gd_{0.02})_{\Sigma 0.95}Ca_{0.05}]^{M1}(Fe^{3+}_{0.42}V^{3+}_{0.34}Al_{0.18}Ti^{4+}_{0.06})^{M2}(Al_{0.96}Fe^{3+}_{0.04})^{M3}(Mn^{2+}_{0.50}Fe^{2+}_{0.43}Mg_{0.07})(SiO_4)(Si_2O_7)O(OH)$. Ferriandrosite-(La), ideally $^{A1}Mn^{2+A2}La^{M1}Fe^{3+M2}Al^{M3}Mn^{2+}(SiO_4)(Si_2O_7)O(OH)$ (Z = 2, space group $P2_1/m$), is the $^{M1}Fe^{3+}$ analogue of androsite. The unit-cell parameters are a = 8.8779(1), b = 5.73995(1), c = 10.0875(2) Å, β = 113.899(1)° and V = 469.97(2) Å^3, and the structural formula is $^{A1}(Mn^{2+}_{0.56}Ca_{0.44})^{A2}[(La_{0.49}Ce_{0.20}Pr_{0.08}Nd_{0.19}Gd_{0.02})_{\Sigma 0.97}Ca_{0.03}]^{M1}(Fe^{3+}_{0.40}V^{3+}_{0.28}Al_{0.20}Fe^{2+}_{0.05}Ti^{4+}_{0.07})^{M2}(Al_{0.97}Fe^{3+}_{0.03})^{M3}(Mn^{2+}_{0.50}Fe^{2+}_{0.40}Mg_{0.10})(SiO_4)(Si_2O_7)O(OH)$ (R_1 = 2.93%). The two new minerals, which are compositionally very similar overall, are distinguished by occupancy of $A1$, Ca *vs.* Mn^{2+}. The structural properties of these minerals depend not only on the *REE* content at $A2$, but also on the Mn content at $A1$.

Keywords: ferriakasakaite-(La), ferriandrosite-(La), lanthanum, epidote supergroup, new minerals.

Introduction

Epidote-supergroup minerals occur in a variety of rock types and geological settings. Among them, the allanite-group minerals are an important class of the rock-forming minerals as a reservoir of rare-earth elements (*REE*) (Gieré and Sorensen, 2004). Stratiform ferromanganese deposits in Japan are reported to be rich in *REE* (Kato *et al*., 2005; Moriyama *et al*., 2010; Fujinaga *et al*., 2011), yet minerals containing *REE* as essential constituents are rare in these deposits. In the present study of *REE*-bearing minerals in a stratiform ferromanganese deposit, we found two new allanite-group minerals from the Shobu area, Ise City, Mie Prefecture, Japan, from which the V-rich allanite-group mineral vanadoallanite-(La) (IMA2012-095), has been reported (Nagashima *et al*., 2013).

The structural formula of monoclinic epidote-supergroup minerals is represented as $A1A2M1M2M3(SiO_4)(Si_2O_7)O(OH)$. The structure consists of a single chain of edge-sharing $M2$ octahedra and a zig-zag chain of central $M1$ octahedra with $M3$ octahedra attached on alternate

* E-mail: nagashim@yamaguchi-u.ac.jp
DOI: 10.1180/minmag.2015.079.3.16

sides along its length. Chains of octahedra run parallel to the *b* axis, linked by SiO_4 and Si_2O_7 groups (Ito *et al*., 1954; Dollase, 1968). This structural arrangement gives rise to 9-coordinate *A*1 and 10-coordinate *A*2 sites. In epidote-group minerals (Mills *et al*., 2009) corresponding to the clinozoisite subgroup defined by Armbruster *et al*. (2006), *A*1 and *A*2 are filled with Ca, and the octahedral *M*1, *M*2 and *M*3 sites are occupied by trivalent cations. Cations having large ionic radii, such as Sr and Ba, occupy *A*2, and those smaller than Ca, such as Mn^{2+}, substitute for Ca at *A*1. On the other hand, the allanite group is defined by a heterovalent substitution of the type $Ca^{2+}(A2) + Me^{3+}(M3) \leftrightarrow REE^{3+}(A2) + Me^{2+}(M3)$ (Armbruster *et al*., 2006). For members of the allanite-group minerals the Levinson-type suffix designation is used to characterize the dominant *REE*, such as La^{3+}, Ce^{3+} and Nd^{3+}.

Two new allanite-group minerals, ferriakasakaite-(La) and ferriandrosite-(La), from the ferromanganese deposit at Ise were approved as new minerals by the Commission on New Minerals, Nomenclature and Classification (IMA2013-126, 2013-127). The ideal formulae are $^{A1}Ca^{A2}La^{M1}Fe^{3+M2}Al^{M3}Mn^{2+}(SiO_4)(Si_2O_7)O(OH)$ (Z = 2) and $^{A1}Mn^{2+A2}La^{M1}Fe^{3+M2}Al^{M3}Mn^{2+}(SiO_4)(Si_2O_7)O(OH)$ (Z = 2), respectively. Ferriakasakaite-(La) is named in honour of the Japanese mineralogist, Prof. Masahide Akasaka (b. 1950) for his outstanding contribution to mineralogy, especially to the study of rock-forming minerals occurring in Mn-Fe ore deposits and natural and synthetic epidote-supergroup minerals. On the basis of the root name 'akasakaite' given by our study, an allanite-subgroup mineral, ideal formula $CaCeFe^{3+}AlMn^{2+}(Si_2O_7)(SiO_4)O(OH)$, from Kesebol, Västra Götaland, Sweden, described by Bonazzi *et al*. (2009) can be named as 'ferriakasakaite-(Ce)'. The name 'ferriandrosite-(*REE*)' was proposed as one of the possible new roots of the allanite group by Armbruster *et al*. (2006). Type specimens of ferriakasakaite-(La) and ferriandrosite-(La) are deposited in the National Museum of Nature and Science, Tokyo, Japan (NSM M-43919 and M-43920). Here we describe the new minerals and examine their crystal-chemical features.

Occurrence and physical properties

Ferriakasakaite-(La) and ferriandrosite-(La) were found in the stratiform ferromanganese deposit in the Shobu area, Ise City, Mie Prefecture, Japan (Fig. 1). The deposit occurs within the Northern Chichibu Belt, which is mainly composed of Jurassic accretionary complexes (Katoh, 1995). The *REE* contents of the ferromanganese deposits in the Chichibu Belt are characteristically high with a negative Ce anomaly and the La contents attain 402–668 ppm (Kato *et al*., 2005) or 1.57–158 ppm (Fujinaga *et al*., 2006) which caused high La and low Ce contents in the epidote-supergroup minerals of the ore deposits in this district.

The manganese ore samples are dark brown to black in colour, and networks of white (<4 mm wide) and pale brown (<2 mm wide) veinlets are often observed. The ores consist mainly of magnetite, hematite and caryopilite. Monazite-(La), chalcopyrite and Ni-Fe sulfides such as pentlandite and heazlewoodite are minor ore minerals. Veinlets are composed mainly of rhodochrosite, bementite, tephroite and calcite (Fig. 2). Allanite-group minerals occur in these veinlets.

The allanite-group minerals are characterized by high La content, and classified as ferriallanite-(La), ferriakasakaite-(La), ferriandrosite-(La) and vanadoallanite-(La). Relative abundances are ferriallanite-(La) > ferriakasakaite-(La), ferriandrosite-(La) >> vanadoallanite-(La). They are indistinguishable macroscopically or by optical microscopy. Thus, precise and accurate chemical and structural analyses are essential for their identification. Ferriakasakaite-(La) and ferriandrosite-(La) occur in veinlets consisting mainly of tephroite ± calcite (Fig. 2) together with the

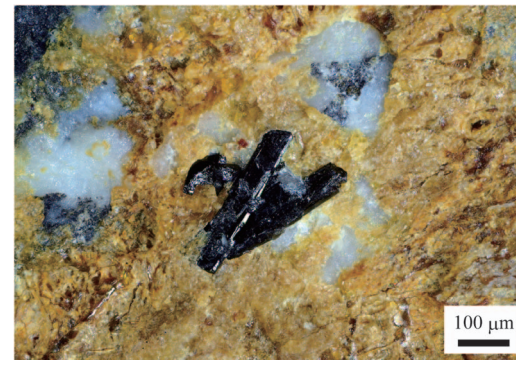

FIG. 1. Representative occurrence of allanite-group minerals (black crystals) in tephroite (yellow) ± calcite (white) veinlet. The photo was taken in plane-polarized light.

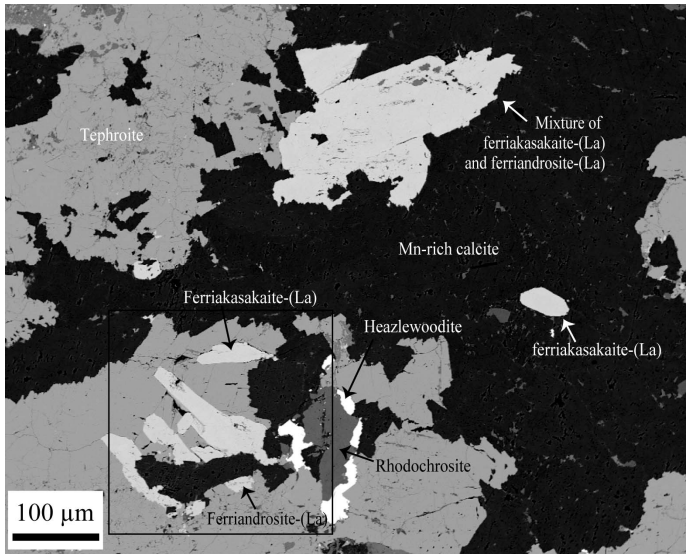

FIG. 2. Backscatter electron image of ferriakasakaite-(La) and ferriandrosite-(La), and associated minerals such as tephroite, calcite, rhodochrosite and heazlewoodite. The square is the area for mapping analysis shown in Fig. 3.

vanadoallanite-(La) reported by Nagashima *et al.* (2013). In addition, iseite $Mn_2Mo_3O_8$ (IMA2012-020), which is an uncommon Mo-Mn mineral, was found in the rhodochrosite veinlets (Nishio-Hamane *et al.*, 2013).

Euhedral to subhedral prismatic crystals elongated parallel to [010] represent the most common appearance of ferriakasakaite-(La) and ferriandrosite-(La). They often form aggregates. Crystals are dark brown with a vitreous lustre (Fig. 1). The length of the crystals varies from several μm to 150 μm. The mineral is brittle with imperfect cleavage on {001}. The calculated densities of ferriakasakaite-(La) and ferriandrosite-(La) are 4.22 and 4.23 g cm^{-3}, respectively.

Experimental

Electron microprobe analysis (EMPA)

The chemical compositions of the crystals studied were determined using a JEOL JXA-8230 electron microprobe analyser at the Centre for Instrumental Analysis, Yamaguchi University. Several crystals were picked from the hand specimen and mounted separately in resin for chemical analysis. Operating conditions were accelerating voltage of 15 kV, beam current of 20 nA and beam diameter of 1 μm. Wavelength dispersive X-ray spectra were measured with LiF, PET and TAP monochromators to identify interfering elements and locate the best wavelengths for background measurements. The abundances of Si, Ti, Al, Cr, V, Fe, Mn, Ni, Mg, Ca, Sr, Ba, Na, K, Y, F, Cl and *REE* (La, Ce, Pr, Nd, Sm, Eu, Gd, Dy, Ho and Er) were measured. Peak and background positions of each element were carefully confirmed to avoid overlap. Several elements, which are not shown in Table 1, were below detection limits. The probe standards for the measured elements excluding *REE* are as follows; wollastonite (Si, Ca), rutile (Ti), corundum (Al), eskolaite (Cr), $Ca_3(VO_4)_2$ (V), hematite (Fe), manganosite (Mn), NiO (Ni), periclase (Mg), $SrBaNb_4O_{12}$ (Sr, Ba), albite (Na), K-feldspar (K), fluorite (F) and halite (Cl). The following standards and X-rays for *REE* were used: synthetic *REE*-bearing hexaborides, $REEB_6$, for La$L\alpha_1$, Ce$L\alpha_1$, Pr$L\beta_1$ and Nd$L\alpha_1$; synthetic *REE*-bearing phosphate standards for Sm$L\beta_1$, Eu$L\alpha_1$, Gd$L\alpha_1$, Dy$L\alpha_1$, Ho$L\alpha_1$ and Er$L\alpha_1$; $(Zr,Y)O_2$ for Y$L\alpha_1$. The measured intensities of Eu$L\alpha_1$ and Gd$L\alpha_1$ were corrected for peak overlap interference of Pr$L\beta_2$ for Eu and La$L\beta_2$ and Ce$L\gamma_1$ for Gd using JEOL software. The *ZAF* correction method was used for all elements. FeO and Fe_2O_3 were calculated based on charge balance where the total positive charge = 25. The difference between analytical total and 100 wt.% was assumed to be H_2O. Table 1 gives the chemical compositions of ferriakasakaite-(La) and ferriandrosite-(La) crystals used for structural analyses.

TABLE 1. Chemical compositions (wt.%) of ferriakasakaite-(La) and ferriandrosite-(La) crystals used for single-crystal X-ray analysis.

	Ferriakasakaite-(La)					Ferriandrosite-(La)					
	1	2	3	Av.	SD	1	2	3	Av.	SD	Probe standard
SiO_2	29.11	29.30	29.04	29.15	0.13	29.05	29.54	29.15	29.25	0.26	$CaSiO_3$
TiO_2	0.71	0.80	0.76	0.75	0.05	1.07	0.90	0.62	0.86	0.22	TiO_2
Al_2O_3	9.36	9.28	9.43	9.35	0.08	9.58	9.58	9.66	9.61	0.04	Al_2O_3
Cr_2O_3	0.08	0.05	0.06	0.06	0.02	0.09	0.12	0.02	0.08	0.05	Cr_2O_3
V_2O_3*1	3.96	4.19	4.18	4.11	0.13	3.53	3.35	3.31	3.40	0.12	$Ca_3(VO_4)_2$
Fe_2O_3*2	5.94	5.18	6.77	5.96	0.79	5.59	5.23	5.61	5.48	0.21	Fe_2O_3
FeO*2	4.77	5.94	4.45	5.05	0.79	5.45	5.36	4.88	5.23	0.31	
MnO*1	11.55	9.98	11.18	10.90	0.82	11.89	11.41	12.85	12.05	0.73	MnO
NiO	0.05	0.01	0.02	0.03	0.02	0.00	0.00	0.05	0.02	0.03	NiO
MgO	0.45	0.48	0.44	0.46	0.02	0.66	0.71	0.58	0.65	0.07	MgO
CaO	5.07	5.57	5.49	5.38	0.27	4.15	4.86	3.77	4.26	0.55	$CaSiO_3$
SrO	0.00	0.02	0.01	0.01	0.01	0.01	0.10	0.00	0.04	0.06	$SrBaNb_4O_{12}$
BaO	0.00	0.02	0.03	0.02	0.02	n.d.	n.d.	n.d.			$SrBaNb_4O_{12}$
K_2O	0.00	0.04	0.05	0.03	0.03	n.d.	n.d.	n.d.			$KAlSi_3O_8$
P_2O_5	0.00	0.05	0.05	0.03	0.03	n.d.	n.d.	n.d.			$KTiOPO_4$
Y_2O_3	0.07	0.00	0.03	0.03	0.04	0.00	0.00	0.02	0.01	0.01	$(Zr,Y)O_2$
La_2O_3	13.06	13.11	12.01	12.73	0.62	12.34	13.57	12.99	12.97	0.62	LaB_6
Ce_2O_3	5.31	5.22	5.22	5.25	0.05	5.24	5.14	5.36	5.25	0.11	CeB_6
Pr_2O_3	1.80	2.09	1.90	1.93	0.15	2.11	1.92	2.11	2.05	0.11	PrB_6
Nd_2O_3	4.99	4.62	5.29	4.97	0.34	5.37	4.72	5.38	5.16	0.38	NdB_6
Gd_2O_3	0.56	0.49	0.48	0.51	0.04	0.65	0.50	0.28	0.48	0.19	GdP_5O_{14}
Er_2O_3	0.04	0.16	0.06	0.09	0.07	0.00	0.00	0.04	0.01	0.02	ErP_5O_{14}
F	0.02	0.08	0.05	0.05	0.03	0.30	0.27	0.28	0.28	0.01	CaF_2
−O=F	−0.01	−0.04	−0.02	−0.02		−0.12	−0.11	−0.12	−0.12		
Total	96.88	96.62	96.98	96.83		96.95	97.17	96.85	96.99		
H_2O (calc.)*3	3.12	3.38	3.02	3.17		3.05	2.83	3.15	3.01		
Total cations = 8											
Si	3.00	3.02	2.97	2.99	0.02	2.99	3.02	3.01	3.01	0.02	
Ti	0.05	0.06	0.06	0.06	0.00	0.08	0.07	0.05	0.07	0.02	
Al	1.13	1.13	1.14	1.13	0.01	1.16	1.16	1.18	1.17	0.01	
Cr	0.01	0.00	0.00	0.01	0.00	0.01	0.01	0.00	0.00	0.01	
V^{3+}	0.33	0.35	0.34	0.34	0.01	0.29	0.28	0.27	0.28	0.01	
Fe^{3+}	0.46	0.40	0.52	0.46	0.06	0.43	0.40	0.44	0.43	0.02	
Fe^{2+}	0.41	0.51	0.38	0.43	0.07	0.47	0.46	0.42	0.45	0.03	

Mn^{2+}	1.01	0.87	0.97	0.95	0.07	1.04	0.99	1.13	1.05	0.07
Ni	0.00	0.00	0.00	0.00	0.00	0.00	0.00	0.00	0.00	0.00
Mg	0.07	0.07	0.07	0.07	0.00	0.10	0.11	0.09	0.10	0.01
Ca	0.56	0.61	0.60	0.59	0.03	0.46	0.53	0.42	0.47	0.06
Sr	0.00	0.00	0.00	0.00	0.00	0.00	0.01	0.00	0.00	0.01
Ba	0.00	0.00	0.00	0.00	0.00					
K	0.00	0.01	0.01	0.00	0.00					
P	0.00	0.00	0.00	0.00	0.00					
Y	0.00	0.00	0.00	0.00	0.00	0.00	0.00	0.00	0.00	0.00
La	0.50	0.50	0.45	0.48	0.03	0.47	0.51	0.50	0.49	0.02
Ce	0.20	0.20	0.20	0.20	0.00	0.20	0.19	0.20	0.20	0.01
Pr	0.07	0.08	0.07	0.07	0.01	0.08	0.07	0.08	0.08	0.01
Nd	0.18	0.17	0.19	0.18	0.01	0.20	0.17	0.20	0.19	0.02
Gd	0.02	0.02	0.02	0.02	0.00	0.02	0.02	0.01	0.01	0.01
Er	0.00	0.01	0.00	0.00	0.00	0.00	0.00	0.00	0.00	0.00
Total	8.00	8.00	8.00	8.00		8.00	8.00	8.00	8.00	
F^-	0.00	0.03	0.02	0.02	0.01	0.10	0.09	0.09	0.09	0.00
OH^-	1.07	1.16	1.03	1.09		1.05	0.97	1.09	1.04	

*[1] V and Mn as V_2O_3 and MnO, respectively.
*[2] FeO and Fe_2O_3 are calculated on the basis of charge balance, total positive charge = 25.
*[3] The difference between the analytical total and 100 wt.% was assumed to be the H_2O content.
SD – standard deviation; nd – not determined.

Single-crystal structure analysis

The X-ray diffraction (XRD) data for single crystals were collected using a Bruker SMART APEX II CCD diffractometer at Shimane University, Japan. The crystals (0.06 mm × 0.04 mm × 0.02 mm for ferriakasakaite-(La) and 0.04 mm × 0.04 mm × 0.04 mm for ferriandrosite-(La)) were picked from the thin section and mounted on a glass fibre. Intensity data were measured at room temperature using graphite-monochromatized Mo*K*α radiation (λ = 0.71069 Å). Preliminary lattice parameters and an orientation matrix were obtained from twelve sets of frames and refined during the integration process of the intensity data. Diffraction data were collected with ω scans at different φ settings (φ−ω scan) (Bruker, 1999). Data were processed using *SAINT* (Bruker, 1999). An empirical absorption correction using *SADABS* (Sheldrick, 1996) was applied. Reflection statistics and systematic absences were consistent with space groups $P2_1$ and $P2_1/m$. Subsequent attempts to solve the structure indicated that the observed structure is centrosymmetric and for this reason $P2_1/m$ is the correct space group. Refinement was performed using *SHELXL-97* (Sheldrick, 2008). Scattering factors for neutral atoms were employed. The position of the hydrogen atom of the hydroxyl group was derived from difference Fourier syntheses. Subsequently, the hydrogen position was refined at a fixed value of U_{iso} = 0.05 Å^2. To obtain the site-scattering values of each cation site, site occupancies were refined with Ca and Mn for *A*1, La for *A*2 (without restraint), Fe and Al for *M*1, Al and Fe for *M*2 and Mn for *M*3 (without restraint). The site occupancies at Si1, Si2 and Si3 were fixed as 1.0 Si, because their occupancies at the preliminary stage indicated that these three sites are fully occupied with Si within error. Final cation assignments were determined using the average chemical compositions of each measured crystal. The hydrogen position was refined with a bond distance constraint of O−H = 0.980(1) Å (Franks, 1973).

Calculated powder diffraction patterns with Cu*K*α radiation were obtained by *RIETAN-FP* (Izumi and Momma, 2007) on the basis of the unit-cell dimensions and atom parameters from the single-crystal analyses, as there was not enough sample for powder XRD measurements.

Results

Chemical compositions of ferriakasakaite-(La) and ferriandrosite-(La)

The chemical compositions of the selected ferriakasakaite-(La) and ferriandrosite-(La) crystals used for single-crystal X-ray analysis are given in Table 1, where the total number of cations, except H, was normalized to eight. Both are characterized by very large MnO and La_2O_3 contents. Although the dominant *REE* is lanthanum in both specimens, they are also rich in Nd and Ce (~5.4 wt.% Ce_2O_3, ~5.4 wt.% Nd_2O_3). The CaO content in ferriakasakaite-(La) (Av. 5.4 wt.%) is larger than in ferriandrosite-(La) (Av. 4.3 wt.%). The corresponding chemical formulae based on average chemical data (n = 3 for each crystal) are $(Ca_{0.59}La_{0.48}Ce_{0.20}Pr_{0.07}Nd_{0.18}Gd_{0.02}Mn^{2+}_{0.45})_{\Sigma 1.99}(Mn^{2+}_{0.50}Mg_{0.07}Fe^{2+}_{0.43}Fe^{3+}_{0.46}V^{3+}_{0.34}Cr_{0.01}Al_{1.13}Ti_{0.06})_{\Sigma 3.00}Si_{2.99}O_{12}(OH)_{1.09}F_{0.02}$ for ferriakasakaite-(La) and $(Ca_{0.47}La_{0.49}Ce_{0.20}Pr_{0.08}Nd_{0.19}Gd_{0.01}Mn^{2+}_{0.55})_{\Sigma 1.99}(Mn^{2+}_{0.50}Mg_{0.10}Fe^{2+}_{0.45}Fe^{3+}_{0.43}V^{3+}_{0.28}Al_{1.17}Ti_{0.07})_{\Sigma 3.00}Si_{3.01}O_{12}(OH)_{1.04}F_{0.09}$ for ferriandrosite-(La). The Fe^{2+}/total Fe values [0.48 for ferriakasakaite-(La) and 0.51 for ferriandrosite-(La)] were calculated based on total positive charge of 25 to maintain charge balance. Mössbauer spectra could not be measured due to the limited amount of sample available. The simplified formulae are $CaLa^{3+}Fe^{3+}AlMn^{2+}(Si_2O_7)(SiO_4)O(OH)$ for ferriakasakaite-(La), which requires SiO_2 29.55, Al_2O_3 8.36, Fe_2O_3 13.09, MnO 11.63, CaO 9.19, La_2O_3 26.71, H_2O 1.48, total 100 wt.% and $Mn^{2+}La^{3+}Fe^{3+}AlMn^{2+}(Si_2O_7)(SiO_4)O(OH)$ for ferriandrosite-(La), which requires SiO_2 28.85, Al_2O_3 8.16, Fe_2O_3 12.78, MnO 22.70, La_2O_3 26.07, H_2O 1.44, total 100 wt.%.

The *REE*, Ca, Fe and Mn contents in both minerals vary in a narrow range. Small chemical variations of Ca, Fe, Mn, V and Al are shown in the X-ray maps of ferriakasakaite-(La) and ferriandrosite-(La) in a thin section (Figs 3*b*–*f*, respectively), from which crystals for the XRD analyses were separated. There tends to be large amounts of Mn^{2+} in the Ca-poor part (Figs 3*b* and *d*), and an enrichment in V^{3+} in the Ca-rich region (Figs 3*b* and *e*). The Al content tends to be large in the most Mn^{2+}-rich area (Figs 3*d* and *f*). The variation of Fe content (Fig. 3*c*) may affect the Fe^{2+}/total Fe ratio.

In spite of such complicated compositional variations, the standard deviations representing the ranges of chemical variation of each crystal

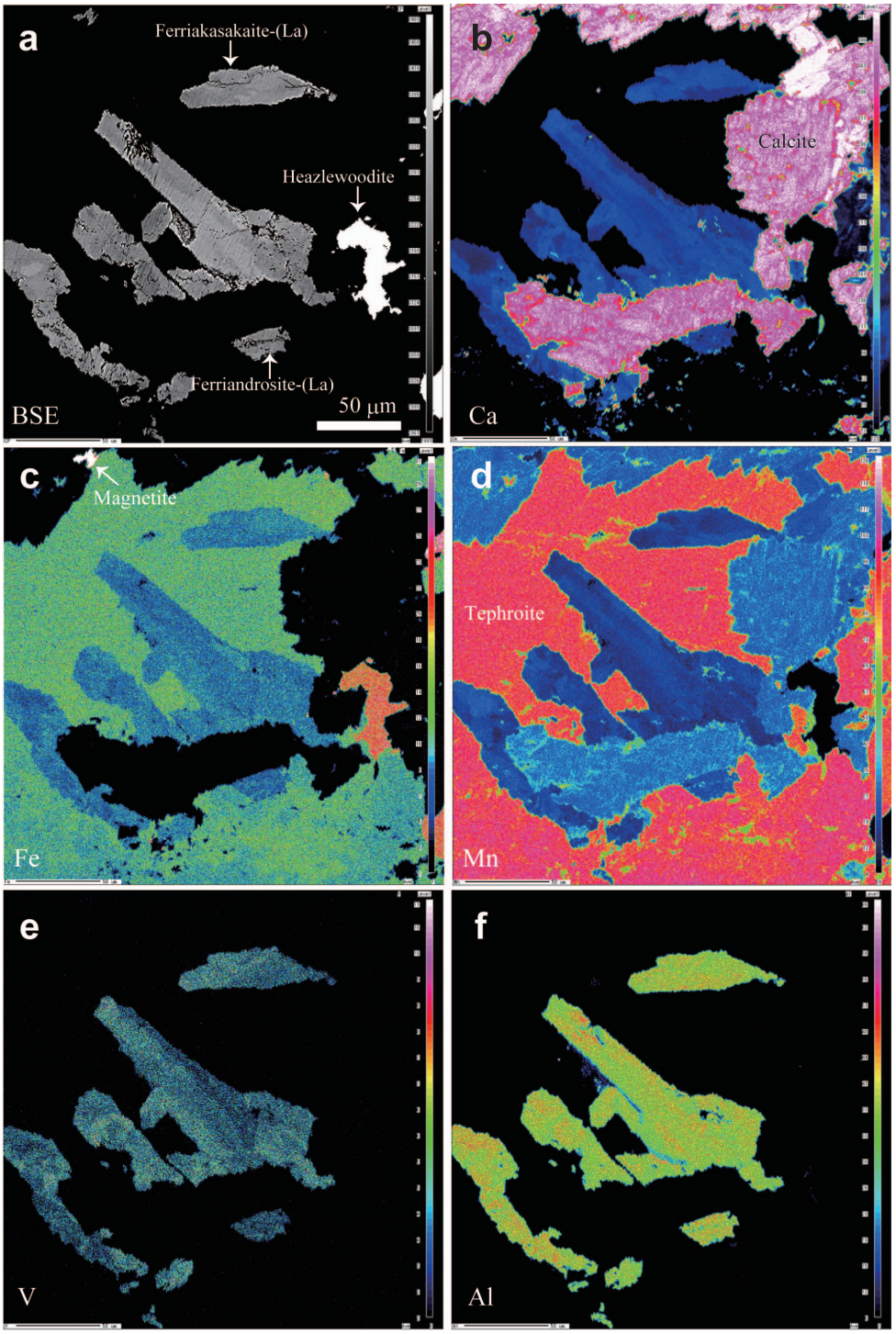

FIG. 3. Backscatter electron image (*a*) and X-ray maps showing the distribution of Ca (*b*), Fe (*c*), Mn (*d*), V (*e*) and Al (*f*) of ferriakasakaite-(La) and ferriandrosite-(La) and their associated minerals.

are not significant (± 0.82 wt.% at maximum, Table 1). Thus it is concluded that the chemical composition of each crystal is represented by the average compositions listed in Table 1.

Crystal-structure refinements and determination of site occupancies

Crystallographic data and refinement parameters are summarized in Table 2. Refined atom positions and anisotropic displacement parameters are listed in Tables 3 and 4 (deposited with the Principal Editor of *Mineralogical Magazine* and available from www.minersoc.org/pages/e_journals/dep_mat_mm.html). Interatomic distances, selected angles and distortions of octahedral sites are presented in Table 5. The crystal structure of ferriakasakaite-(La) and ferriandrosite-(La) is shown in Fig. 4. Calculated powder diffraction data are listed in Table 6.

Observed and estimated electron numbers and the determined site occupancies are listed in Table 7. Occupancies of cation sites were calculated by following procedure: (1) elements <0.01 a.p.f.u. in EMPA data were omitted; (2) octahedral cations except for Al, such as Fe, Mn, V and Ti, were treated as Fe or Mn in the refinement; (3) The sum of $A1 + A2 + M1 + M2 + M3$ was normalized to five with recalculated Fe^{2+} and Fe^{3+} values; (4) V^{3+} was treated as Fe^{3+}, because the site distribution of V^{3+} ions was unknown. Among the *REE*, La, Ce, Pr and Gd, occupying *A*2, La is the dominant cation at *A*2 in both minerals. Calcium ions partially occupy *A*1 and *A*2. The number of electrons at *A*1 is obviously >20 because Mn^{2+} ions compensate

TABLE 2. Data-collection and structure-refinement details.

		Ferriakasakaite-(La)	Ferriandrosite-(La)
Space group		$P2_1/m$	$P2_1/m$
Crystal size (mm)		0.06 × 0.04 × 0.02	0.04 × 0.04 × 0.04
Cell parameters	*a* (Å)	8.8733(2)	8.8779(1)
	b (Å)	5.7415(1)	5.7399(1)
	c (Å)	10.0805(3)	10.0875(2)
	β (°)	113.845(2)	113.899(1)
	V (Å^3)	469.73(2)	469.97(2)
*D*calc (g cm^{-3})		4.35	4.35
Absorption coefficient (mm^{-1})		8.62	8.61
Collected reflections		4386	9217
Unique reflections		1500	2733
R_{int} (%)		4.16	3.01
R_σ (%)		4.83	4.23
θ_{max} (°)		30.0	38.9
Miller index limit		$-12 \leqslant h \leqslant 12$, $-7 \leqslant k \leqslant 8$, $-13 \leqslant 1 \leqslant 14$	$-15 \leqslant h \leqslant 14$, $-8 \leqslant k \leqslant 9$, $-17 \leqslant l \leqslant 17$
R_1 (%)		3.13	2.93
wR_2 (%)		6.23	5.81
S		1.01	1.01
No. of parameters		125	125
Weighting scheme		$w = 1/[\sigma^2(F_o^2) + (0.0270P)^2]$	$w = 1/[\sigma^2(F_o^2) + (0.0264P)^2]$
$\Delta\rho_{max}$ (e Å^{-3})		1.01 (0.59 Å from O9)	1.25 (0.76 Å from Si2)
$\Delta\rho_{min}$ (e Å^{-3})		−1.02 (0.74 Å from *A*2)	−1.23 (0.55 Å from Si1)

The XRD data were collected using a Bruker SMART APEX II CCD diffractometer. Intensity data were measured at room temperature using graphite-monochromatized Mo*K*α radiation (λ = 0.71069 Å). Diffraction data were collected with φ-ω scan (Bruker, 1999). Data were processed using *SAINT* (Bruker, 1999). An empirical absorption correction using *SADABS* (Sheldrick, 1996) was applied. Structural refinement was performed using *SHELXL-97* (Sheldrick, 2008). The function of the weighting scheme is $w = 1/[\sigma^2(Fo^2) + (a{\cdot}P)^2 + b{\cdot}P]$, where $P = [\mathrm{Max}(Fo^2, 0)+2Fc^2]/3$, and the parameters *a* and *b* are chosen to minimize the differences in the variances for reflections in different ranges of intensity and diffraction angle.

TABLE 3. Refined atom positions and isotropic displacement parameters (Å^2).

Site	W*		Ferriakasakaite-(La)	Ferriandrosite-(La)	Site	W*		Ferriakasakaite-(La)	Ferriandrosite-(La)
$A1$	2e	x/a	0.76007(13)	0.76004(7)	O3	4f	x/a	0.8015(3)	0.80141(19)
		y/b	¾	¾			y/b	0.0121(5)	0.0126(3)
		z/c	0.15183(12)	0.15192(6)			z/c	0.3320(3)	0.33218(18)
		U_{eq}	0.0130(3)	0.01249(14)			U_{eq}	0.0128(7)	0.0122(3)
$A2$	2e	x/a	0.59357(4)	0.59324(2)	O4	2e	x/a	0.0580(5)	0.0575(3)
		y/b	¾	¾			y/b	¼	¼
		z/c	0.42829(4)	0.428109(19)			z/c	0.1371(4)	0.1367(2)
		U_{eq}	0.01063(11)	0.00996(5)			U_{eq}	0.0131(9)	0.0120(4)
$M1$	2b	x/a	0	0	O5	2e	x/a	0.0495(5)	0.0495(3)
		y/b	0	0			y/b	¾	¾
		z/c	0	0			z/c	0.1560(4)	0.1564(2)
		U_{eq}	0.0092(3)	0.00855(16)			U_{eq}	0.0123(9)	0.0116(4)
$M2$	2a	x/a	0	0	O6	2e	x/a	0.0776(5)	0.0773(3)
		y/b	0	0			y/b	¾	¾
		z/c	½	½			z/c	0.4192(4)	0.4188(2)
		U_{eq}	0.0078(5)	0.0068(2)			U_{eq}	0.0116(8)	0.0109(4)
$M3$	2c	x/a	0.31095(10)	0.31047(6)	O7	2e	x/a	0.5136(5)	0.5142(3)
		y/b	¼	¼			y/b	¾	¾
		z/c	0.20996(10)	0.20997(5)			z/c	0.1759(5)	0.1761(2)
		U_{eq}	0.0117(3)	0.01123(14)			U_{eq}	0.0142(9)	0.0141(5)
Si1	2e	x/a	0.34513(19)	0.34536(11)	O8	2e	x/a	0.5523(5)	0.5521(3)
		y/b	¾	¾			y/b	¼	¼
		z/c	0.03451(17)	0.03459(9)			z/c	0.3433(5)	0.3434(3)
		U_{eq}	0.0090(4)	0.00875(17)			U_{eq}	0.0191(11)	0.0180(5)
Si2	2e	x/a	0.69200(18)	0.69168(10)	O9	2e	x/a	0.6042(5)	0.6036(3)
		y/b	¼	¼			y/b	¼	¼
		z/c	0.28134(18)	0.28127(9)			z/c	0.1037(5)	0.1039(2)
		U_{eq}	0.0092(4)	0.00833(17)			U_{eq}	0.0164(10)	0.0153(5)
Si3	2e	x/a	0.19090(18)	0.19111(10)	O10	2e	x/a	0.0902(5)	0.0906(3)
		y/b	¾	¾			y/b	¼	¼
		z/c	0.32433(17)	0.32490(9)			z/c	0.4316(5)	0.4314(2)
		U_{eq}	0.0083(4)	0.00781(16)			U_{eq}	0.0119(8)	0.0098(4)
O1	4f	x/a	0.2403(3)	0.24029(19)	H10	2e	x/a	0.058(10)	0.053(6)
		y/b	0.9895(5)	0.9894(3)			y/b	¼	¼
		z/c	0.0231(3)	0.02320(18)			z/c	0.3265(14)	0.3257(7)
		U_{eq}	0.0143(7)	0.0138(3)			U_{iso}	0.05	0.05
O2	4f	x/a	0.3154(3)	0.31587(19)					
		y/b	0.9711(5)	0.9714(3)					
		z/c	0.3633(3)	0.36375(17)					
		U_{eq}	0.0119(6)	0.0104(3)					

* W = Wyckoff notation of point position with multiplicity.

TABLE 5. Selected interatomic distances (Å), angles (°), volume of polyhedra (Å^3) and distortion parameters for the octahedral sites*.

	Ferriakasakaite-(La)	Ferriandrosite-(La)		Ferriakasakaite-(La)	Ferriandrosite-(La)		Ferriakasakaite-(La)	Ferriandrosite-(La)
*A*1– O1 ×2	2.312(3)	2.314(2)	*M*1–O1 ×2	2.050(3)	2.050(2)	O1–*M*1–O4	88.6(1)	88.77(8)
O3 ×2	2.272(3)	2.274(2)	O4 ×2	1.913(3)	1.911(2)	O1–*M*1–O5	90.1(1)	90.14(8)
O5	2.552(4)	2.552(2)	O5 ×2	2.042(3)	2.045(2)	O4–*M*1–O5	93.4(1)	93.39(7)
O7	2.296(4)	2.292(3)	Av.	2.002	2.002			
Av.	2.335	2.337	$V^{M1(VI)}$ (Å^3)	10.65	10.66	O3–*M*2–O6	89.3(2)	89.34(8)
O6	3.011(4)	3.006(2)	*DI* (oct)	0.029	0.030	O3–*M*2–O10	91.4(2)	91.37(8)
O9 ×2	3.138(2)	3.1393(9)	<λ oct>	1.003	1.003	O6–*M*2–O10	97.8(1)	97.60(7)
Av.	2.589	2.589	σ_q (oct)^2	4.95	4.74			
$V^{A1(VI)}$ (Å^3)	15.64	15.66				O1–*M*3–O1′	81.8(2)	81.77(9)
$V^{A1(IX)}$ (Å^3)	26.42	26.41	*M*2–O3 ×2	1.888(3)	1.887(2)	O1–*M*3–O2	91.3(1)	91.49(6)
			O6 ×2	1.911(3)	1.912(2)	O1–*M*3–O4	79.0(1)	79.09(6)
*A*2– O2 ×2	2.612(3)	2.609(2)	O10 ×2	1.903(3)	1.907(2)	O1–*M*3–O8	114.4(1)	114.25(7)
O2’ ×2	2.502(3)	2.499(2)	Av.	1.901	1.902	O2–*M*3–O2′	92.6(2)	92.44(8)
O3 ×2	2.839(3)	2.841(2)	$V^{M2(VI)}$ (Å^3)	9.07	9.09	O2–*M*3–O4	87.6(1)	87.84(6)
O7	2.349(4)	2.347(2)	*DI* (oct)	0.005	0.005	O2–*M*3–O8	79.6(1)	79.48(6)
O10	2.582(4)	2.582(2)	<λ oct>	1.007	1.006			
Av.	2.605	2.603	σ_θ (oct)^2	22.82	21.73	O1–Si1–O1′	114.2(2)	114.0(1)
O8 ×2	2.976(1)	2.9745(7)				O1–Si1–O7	111.3(1)	111.36(8)
Av.	2.679	2.678	*M*3–O1 ×2	2.286(3)	2.286(2)	O1–Si1–O9	106.6(1)	106.70(8)
$V^{A2(VIII)}$ (Å^3)	28.80	28.76	O2 ×2	2.214(3)	2.215(2)	O7–Si1–O9	106.4(2)	106.2(1)
$V^{A2(X)}$ (Å^3)	38.19	38.13	O4	2.060(4)	2.060(2)			
			O8	2.016(4)	2.018(2)	O3–Si2–O3′	113.4(2)	113.2(1)
Si1– O1 ×2	1.638(3)	1.638(2)	Av.	2.179	2.180	O3–Si2–O8	109.6(1)	109.59(8)
O7	1.595(4)	1.597(2)	$V^{M3(VI)}$ (Å^3)	12.89	12.91	O3–Si2–O9	107.6(2)	107.68(8)
O9	1.627(5)	1.633(3)	*DI* (oct)	0.043	0.043	O8–Si2–O9	109.0(2)	109.0(1)
Av.	1.625	1.627	<λ oct>	1.049	1.049			
$V^{Si1(IV)}$ (Å^3)	2.19	2.20	σ_q (oct)^2	157.66	156.72	O2–Si3–O2’	102.9(2)	102.8(1)
						O2–Si3–O5	114.1(1)	114.04(8)
Si2– O3 ×2	1.634(3)	1.632(2)	Si3–O2 ×2	1.624(3)	1.626(2)	O2–Si3–O6	112.1(1)	112.30(8)
O8	1.598(4)	1.599(3)	O5	1.653(4)	1.655(2)	O5–Si3–O6	102.0(2)	101.8(1)
O9	1.639(5)	1.637(2)	O6	1.645(4)	1.641(2)			
Av.	1.626	1.626	Av.	1.636	1.637	Si1–O9–Si2	139.6(3)	139.4(2)
$V^{Si2(IV)}$ (Å^3)	2.20	2.20	$V^{Si3(IV)}$ (Å^3)	2.22	2.22			
O10···O4	2.865(6)	2.866(3)						

* $DI(\text{oct}) = 1/6\Sigma|R_i - R_{\text{av.}}|/R_{\text{av.}}$ (R_i: each bond length, $R_{\text{av.}}$: average distance for an octahedron) (Baur, 1974); $<\lambda_{\text{oct}}> = \sum_{i=1}^{6}(l_i - l_0)^2/6$ (l_i: each bond length, l_0: centre-to-vertex distance for an octahedron with O_h symmetry, of which the volume is equal to that of a distorted octahedron with bond lengths l_i) (Robinson *et al.*, 1971); and $\sigma_\theta(\text{oct})^2 = \sum_{i=1}^{12}(\theta_i - 90°)^2/11$ (θ_i: O–*M*–O angle) (Robinson *et al.*, 1971).

for the Ca deficiency at *A*1. The numbers of electrons at *A*1 of both minerals are almost identical within error (Table 7), suggesting similar cation populations at *A*1. The difference in average Ca contents of ferriandrosite-(La) (0.42±0.06 a.p.f.u.) and ferriakasakaite-(La) (0.56±0.03 a.p.f.u.) (Table 1) may be attributed to the limited EMPA analysis positions.

The scheme of the site occupancy determination at the octahedral *M*1, *M*2 and *M*3 sites is as follows:

(1) Octahedral divalent cations, Mn^{2+}, Fe^{2+} and Mg are assigned to *M*3 in descending order. In ferriakasakaite-(La), the deficiency at *M*3 is compensated by Fe^{3+}; the small amount of Fe^{2+} (0.05 a.p.f.u.) is assigned to *M*1 in ferriandrosite-(La).

(2) *M*2 is occupied mainly by Al, and small amounts of heavier cations, such as Fe^{3+} and Ti^{4+}, are also assigned to *M*2 based on the number of electrons exceeding 13. In Table 7, two different assignments for *M*2 are given, either Fe^{3+} following Armbruster *et al*. (2006), or Ti^{4+} following Nagashima *et al*. (2011).

(3) Other cations, such as Ti^{4+}, Al^{3+}, Fe^{3+} and V^{3+}, are assigned to *M*1.

As a result, the determined cation distributions at *A*1, *A*2 and *M*3 of ferriakasakaite-(La) are $Ca_{0.54}Mn_{0.46}$, $(La_{0.48}Ce_{0.20}Pr_{0.07}Nd_{0.18}Gd_{0.02})_{\Sigma 0.95}Ca_{0.05}$ and $Mn^{2+}_{0.50}Fe^{2+}_{0.43}Mg_{0.07}$, respectively, and those of ferriandrosite-(La) are $Mn_{0.56}Ca_{0.44}$, $(La_{0.49}Ce_{0.20}Pr_{0.08}Nd_{0.19}Gd_{0.02})_{\Sigma 0.97}Ca_{0.03}$ and $Mn^{2+}_{0.50}Fe^{2+}_{0.40}Mg_{0.10}$, respectively. However, there are two different models for the Ti distribution. The two possible cation assignments at the *M*1 and *M*2 sites are (1) $(Fe^{3+}_{0.42}V^{3+}_{0.34}Al_{0.18}Ti^{4+}_{0.06})^{M1}(Al_{0.96}Fe^{3+}_{0.04})^{M2}$ and (2) $(Fe^{3+}_{0.46}V^{3+}_{0.34}Al_{0.20})^{M1}(Al_{0.94}Ti^{4+}_{0.06})^{M2}$ for ferriakasakaite-(La) and (1) $(Fe^{3+}_{0.40}V^{3+}_{0.28}Al_{0.20}Fe^{2+}_{0.05}Ti^{4+}_{0.07})^{M1}(Al_{0.97}Fe^{3+}_{0.03})^{M2}$ and (2) $(Fe^{3+}_{0.43}V^{3+}_{0.28}Al_{0.21}Fe^{2+}_{0.05}Ti^{4+}_{0.03})^{M1}(Al_{0.96}Ti^{4+}_{0.04})^{M2}$ for ferriandrosite-(La). However, both models lead to the same predominant cations at *A*1, *A*2, *M*1 and *M*3 in these minerals: Ca, La^{3+}, Fe^{3+} and Mn^{2+} for ferriakasakaite-(La), and Mn^{2+}, La^{3+}, Fe^{3+}, Mn^{3+} for ferriandrosite-(La), respectively. In both crystals, some difference between the observed and estimated number of electrons at *M*1 (and *M*3) is striking (Table 7); the observed number of electrons of *M*1 is somewhat smaller than the estimated ones and that of *M*3 is *vice versa*. This is attributed to chemical zonation by the

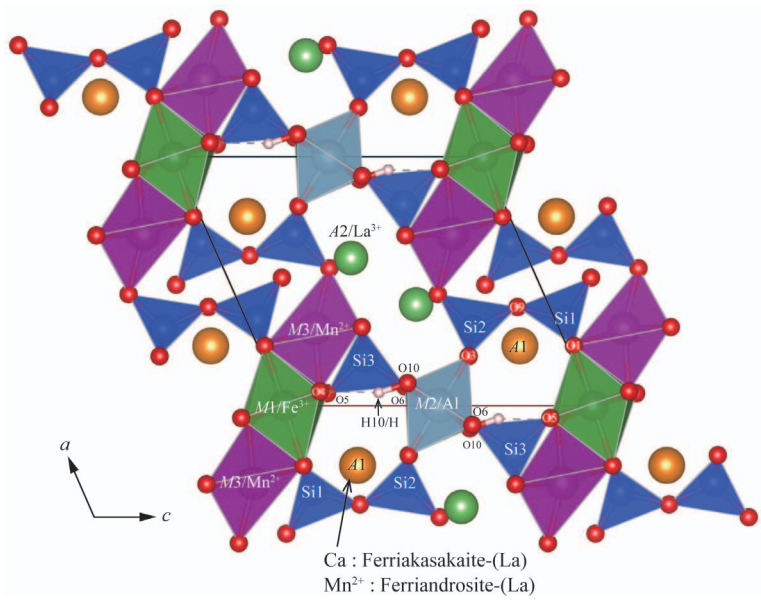

FIG. 4. Crystal structure of ferriakasakaite-(La)/ferriandrosite-(La) projected onto (010) drawn with the program *VESTA3* (Momma and Izumi, 2011). Dashed lines indicate H···O bonds. The dominant cations at *M*1, *M*2, *M*3 and *A*2 are represented with each site name. The difference between ferriakasakaite-(La) and ferriandrosite-(La) is the dominant cation at *A*1. The former is Ca and the latter Mn^{2+}.

TABLE 6. Calculated powder diffraction patterns based on the results of single-crystal X-ray analyses*.

Ferriakasakaite-(La)						Ferriandrosite-(La)					
h	*k*	*l*	2θ (º)	*d* (Å)	I_{calc}	*h*	*k*	*l*	2θ (º)	*d* (Å)	I_{calc}
0	0	1	9.59	9.220	26	0	0	1	9.58	9.223	23
1	0	0	10.89	8.116	18	1	0	0	10.89	8.117	17
1	0	$\bar{1}$	11.23	7.871	23	1	0	$\bar{1}$	11.22	7.878	23
1	0	1	17.22	5.147	18	1	0	1	17.22	5.146	19
1	0	$\bar{2}$	17.86	4.961	8	1	0	$\bar{2}$	17.85	4.965	8
0	1	1	18.19	4.874	7	0	1	1	18.19	4.873	7
1	1	0	18.92	4.687	18	1	1	0	18.92	4.686	18
0	0	2	19.24	4.610	11	0	0	2	19.23	4.611	11
1	1	$\bar{2}$	23.68	3.754	10	1	1	$\bar{2}$	23.67	3.755	10
0	1	2	24.75	3.595	11	0	1	2	24.75	3.595	10
2	1	$\bar{1}$	25.36	3.509	47	2	1	$\bar{1}$	25.36	3.510	46
2	1	0	26.88	3.314	14	2	1	0	26.88	3.314	14
2	0	1	27.34	3.260	12	2	0	1	27.34	3.260	12
2	1	$\bar{2}$	27.45	3.246	5	2	1	$\bar{2}$	27.44	3.248	5
3	0	$\bar{2}$	30.80	2.901	22	3	0	$\bar{2}$	30.78	2.903	22
1	1	$\bar{3}$	30.82	2.899	100	1	1	$\bar{3}$	30.80	2.900	100
0	2	0	31.13	2.871	40	0	2	0	31.14	2.870	40
2	1	1	31.53	2.835	13	2	1	1	31.54	2.834	13
0	2	1	32.64	2.741	5	0	2	1	32.65	2.740	5
0	1	3	33.03	2.710	35	0	1	3	33.03	2.710	35
1	2	0	33.07	2.706	35	1	2	0	33.08	2.706	35
3	0	0	33.09	2.705	12	3	0	0	33.08	2.706	12
3	0	$\bar{3}$	34.15	2.624	6	3	0	$\bar{3}$	34.11	2.626	5
3	1	$\bar{1}$	34.27	2.614	53	3	1	$\bar{1}$	34.27	2.615	53
2	0	2	34.84	2.573	26	2	0	2	34.84	2.573	26
1	0	$\bar{4}$	35.91	2.499	5	1	0	$\bar{4}$	35.89	2.500	5
1	2	$\bar{2}$	36.12	2.485	6	1	2	$\bar{2}$	36.12	2.485	7
0	2	2	36.85	2.437	5	0	2	2	36.86	2.437	5
3	1	$\bar{3}$	37.66	2.386	13	3	1	$\bar{3}$	37.64	2.388	13
2	2	$\bar{2}$	38.80	2.319	13	2	2	$\bar{2}$	38.79	2.320	13
3	0	$\bar{4}$	39.79	2.263	8	3	0	$\bar{4}$	39.76	2.266	8
1	2	2	40.84	2.208	9	1	2	2	40.85	2.207	8
1	2	$\bar{3}$	41.34	2.182	7	1	2	$\bar{3}$	41.33	2.183	7
4	0	$\bar{1}$	41.49	2.175	21	4	0	$\bar{1}$	41.48	2.175	22
2	2	1	41.90	2.154	19	2	2	1	41.91	2.154	19
0	1	4	42.21	2.139	7	0	1	4	42.21	2.140	7
4	0	$\bar{3}$	42.27	2.136	5	4	0	$\bar{3}$	42.24	2.138	5
2	2	$\bar{3}$	42.67	2.117	20	2	2	$\bar{3}$	42.66	2.118	20
0	2	3	43.08	2.098	13	0	2	3	43.08	2.098	14
2	0	3	43.50	2.079	9	2	0	3	43.51	2.079	9
2	2	2	47.41	1.916	15	2	2	2	47.42	1.916	15
1	1	4	47.83	1.900	7	1	1	4	47.83	1.900	7
3	1	2	48.00	1.894	5	3	1	2	48.01	1.893	5
2	2	$\bar{4}$	48.46	1.877	11	2	2	$\bar{4}$	48.44	1.878	12
5	0	$\bar{2}$	51.54	1.772	5	5	0	$\bar{2}$	51.51	1.773	5
2	3	$\bar{1}$	52.00	1.757	7	2	3	$\bar{1}$	52.01	1.757	7
4	2	$\bar{2}$	52.09	1.754	5	4	2	$\bar{2}$	52.07	1.755	5
4	1	$\bar{5}$	54.33	1.687	7	4	1	$\bar{5}$	54.28	1.689	7
2	0	$\bar{6}$	54.60	1.679	5	2	0	$\bar{6}$	54.56	1.681	5
1	3	$\bar{3}$	55.19	1.663	13	1	3	$\bar{3}$	55.20	1.663	13
4	2	0	55.41	1.657	5	4	2	0	55.41	1.657	5
5	1	$\bar{1}$	55.69	1.649	6	5	1	$\bar{1}$	55.67	1.650	6
3	2	2	55.87	1.644	9	1	2	4	55.72	1.648	5

TABLE 6 (*contd.*)

Ferriakasakaite-(La)						Ferriandrosite-(La)					
h	*k*	*l*	2θ (º)	*d* (Å)	I_{calc}	*h*	*k*	*l*	2θ (º)	*d* (Å)	I_{calc}
1	0	$\bar{6}$	56.20	1.636	11	3	2	2	55.88	1.644	9
0	3	3	56.61	1.625	6	1	0	$\bar{6}$	56.17	1.636	11
4	2	$\bar{4}$	56.67	1.623	20	0	3	3	56.62	1.624	6
5	1	$\bar{4}$	56.86	1.618	5	4	2	$\bar{4}$	56.63	1.624	21
3	3	$\bar{1}$	57.43	1.603	12	5	1	$\bar{4}$	56.82	1.619	5
1	1	5	57.80	1.594	9	3	3	$\bar{1}$	57.43	1.603	12
4	1	2	58.85	1.568	9	1	1	5	57.80	1.594	9
4	0	$\bar{6}$	58.87	1.567	7	4	0	$\bar{6}$	58.82	1.569	7
						4	1	2	58.86	1.568	9

* Only reflections with relative intensity >4% are listed.

octahedral cations, such as Fe, Mn, V and Al, which also has an effect on the ionic distribution at *M*1. The observed number of electrons of *M*1 may suggest that the quantity of Mg assigned to *M*1 is slightly underestimated.

Discussion

Relationship between cation distributions and structural variations

Structural variations due to ionic substitutions in minerals affect unit-cell parameters. Based on systematic studies of the synthetic clinozoisite group of the epidote supergroup, in which *A*1, *A*2 and *M*2 are filled with Ca, Ca and Al, respectively, cation distributions at *M*3 and *M*1 strongly influence the *a* , *b* and *c* dimensions but not the β angle (115.5±0.2º) (Anastasiou and Langer, 1977; Giuli *et al*., 1999; Langer *et al*., 2002; Nagashima and Akasaka, 2004; Nagashima *et al*., 2009, 2010). On the other hand, *REE* contents at *A*2 in *REE*-bearing epidote-supergroup minerals affect not only the *a*, *b* and *c* dimensions but also the β angle; the latter decreases systematically with increasing *REE* content at *A*2 (Fig. 5*a*), as noted by Bonazzi and Menchetti (1995, 2004) and Gieré and Sorensen (2004). Thus, the β angle is one of the critical parameters indicating structural variation caused by *REE* content at *A*2.

However, as shown in Fig. 5*a*, the β angles plotted against REE^{3+} content at *A*2 of Mn^{2+} *REE*-bearing epidote-supergroup minerals having >0.1 a.p.f.u. Mn^{2+} at *A*1 and >0.1 REE^{3+} at *A*2, are generally smaller than those of Mn^{2+}-free allanite. The β angles *vs.* REE^{3+} content at *A*2 of ferriakasakaite-(La) and ferriandrosite-(La) are also significantly smaller than the values expected using the regression line for Mn^{2+}-free allanite-group minerals (Fig. 5*a*). That is to say, in addition to *REE* content at *A*2, the Mn^{2+} content at *A*1 strongly affects the β angle. In fact, as shown in Fig. 5*b*, the β angles of Mn^{2+}-bearing/rich epidote-supergroup minerals, except for uedaite-(Ce), show a systematic decrease with increasing Mn^{2+} content at *A*1. Such structural variation with the substitution of Mn^{2+} for Ca at *A*1 is caused by a topological change of $A1O_9$ polyhedra, as described by Bonazzi *et al*. (1996) and Nagashima *et al*. (2010, 2013); O3 and O1 (2nd to 5th neighbour oxygen atoms) get closer to *A*1, O6 (7th neighbour) and O9 (8th and 9th neighbours) shift away from *A*1 with increasing Mn^{2+} at *A*1, whereas O5 and O7 positions are not influenced. This results in a positive correlation between δ[(*A*1−O6)−(*A*1−O5)] (Å) and Mn^{2+} at *A*1 (a.p.f.u.), as first pointed out by Bonazzi *et al*. (1996) and confirmed by Nagashima *et al*. (2010, 2013). The δ[(*A*1−O6)−(*A*1−O5)] values of ferriakasakaite-(La) (0.459(3) Å against $Ca_{0.55}Mn_{0.45}$ at *A*1) and ferriandrosite-(La) (0.454(3) Å against $Ca_{0.45}Mn_{0.55}$ at *A*1) are also consistent with those of other epidote-supergroup minerals containing Mn^{2+} at *A*1 [except for uedaite-(Ce)] (Fig. 5). As Mn^{2+} abundance at *A*1 significantly affects the topology of $A1O_9$ polyhedra, the low total Mn^{2+} + Ca content of uedaite-(Ce), ~0.8 a.p.f.u. (Miyawaki *et al*., 2008) may cause the difference of β and δ[(*A*1−O6)−(*A*1−O5)] with respect to other epidote-supergroup minerals with Mn^{2+} at *A*1 (Figs 5 and 6). Large amounts of Al^{3+} at *M*1 in uedaite-(Ce) may also influence β and δ[(*A*1−O6)−(*A*1−O5)]. In Mn^{2+}-free epidote

TABLE 7. Number of electrons and cation-site assignments for ferriakasakaite-(La) and ferriandrosite-(La).*

Site	Observed no. of e^-	Cation assignment based on EMPA	Estimated no. of e^-	Observed no. of e^-	Cation assignment based on EMPA	Estimated no. of e^-
	Ferriakasakaite-(La)			Ferriandrosite-(La)		
*A*1	22.3(4)	$Ca_{0.54}Mn_{0.46}$	22.30	22.2(2)	$Mn_{0.56}Ca_{0.44}$	22.80
*A*2	56.5(2)	$(La_{0.48}Ce_{0.20}Pr_{0.07}Nd_{0.18}Gd_{0.02})_{\Sigma 0.95}Ca_{0.05}$	56.17	56.4(1)	$(La_{0.49}Ce_{0.20}Pr_{0.08}Nd_{0.19}Gd_{0.02})_{\Sigma 0.97}Ca_{0.03}$	56.89
Si1	14	$Si_{1.0}$ (fixed)	14	14	$Si_{1.0}$ (fixed)	14
Si2	14	$Si_{1.0}$ (fixed)	14	14	$Si_{1.0}$ (fixed)	14
Si3	14	$Si_{1.0}$ (fixed)	14	14	$Si_{1.0}$ (fixed)	14
	Case 1 (Fe^{3+} in *M*2)			Case 1 (Fe^{3+} in *M*2)		
*M*1	19.23(8)	$Fe^{3+}_{0.42}V^{3+}_{0.34}Al_{0.18}Ti^{4+}_{0.06}$	22.40	19.88(9)	$Fe^{3+}_{0.40}V^{3+}_{0.28}Al_{0.20}Fe^{2+}_{0.05}Ti^{4+}_{0.07}$	22.28
*M*2	13.52(9)	$Al_{0.96}Fe^{3+}_{0.04}$	13.52	13.35(5)	$Al_{0.97}Fe^{3+}_{0.03}$	13.39
*M*3	25.0(1)	$Mn^{2+}_{0.50}Fe^{2+}_{0.43}Mg_{0.07}$	24.52	24.94(7)	$Mn^{2+}_{0.50}Fe^{2+}_{0.40}Mg_{0.10}$	24.10
	Case 2 (Ti^{4+} in *M*2)			Case 2 (Ti^{4+} in *M*2)		
*M*1	19.23(8)	$Fe^{3+}_{0.46}V^{3+}_{0.34}Al_{0.20}$	22.38	19.88(9)	$Fe^{3+}_{0.43}V^{3+}_{0.28}Al_{0.21}Fe^{2+}_{0.05}Ti^{4+}_{0.03}$	22.31
*M*2	13.52(9)	$Al_{0.94}Ti^{4+}_{0.06}$	13.54	13.35(5)	$Al_{0.96}Ti^{4+}_{0.04}$	13.36
*M*3	25.0(1)	$Mn^{2+}_{0.50}Fe^{2+}_{0.42}Mg_{0.07}$	24.52	24.94(7)	$Mn^{2+}_{0.50}Fe^{2+}_{0.40}Mg_{0.10}$	24.10

* The cation contents are fixed by EMPA data. The Fe^{2+}/Fe^{3+} ratio was estimated based on charge-balance calculations.

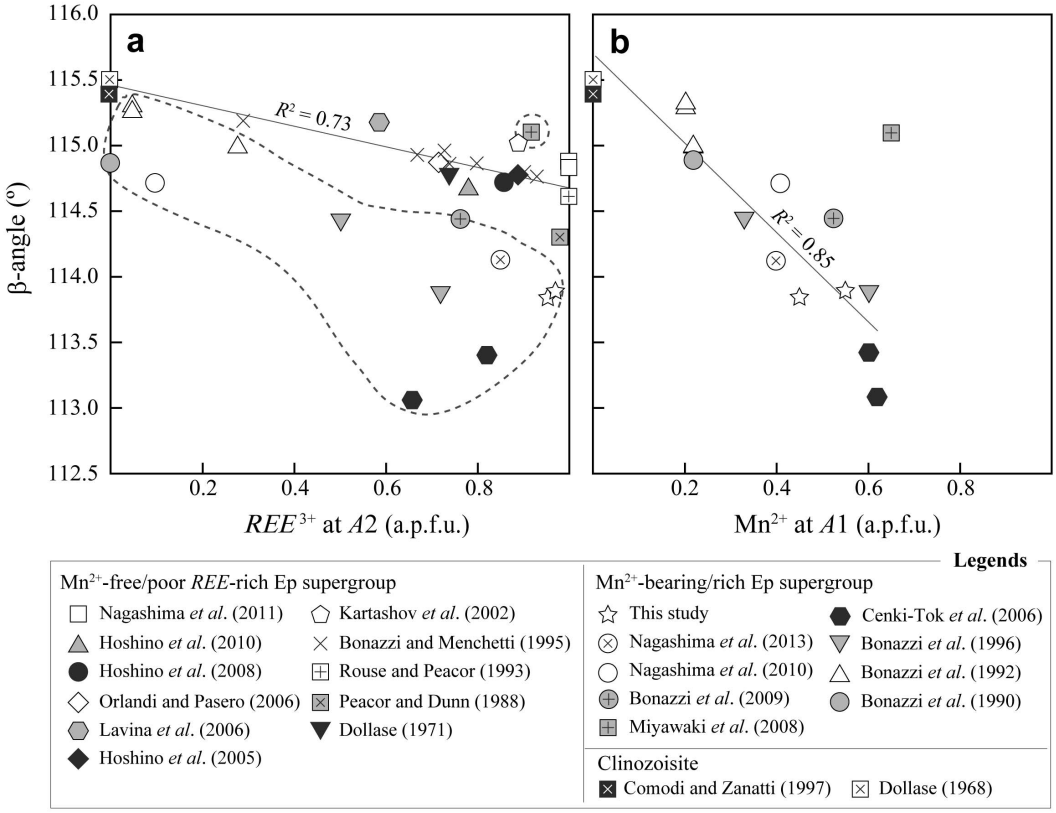

FIG. 5. Variation of the β angle as functions of REE^{3+} at $A2$ (*a*) and Mn^{2+} at $A1$ (*b*). Symbols surrounded by dashed lines in Fig. 4*a* are Mn^{2+}-bearing/rich epidote-supergroup minerals. The regression functions are (*a*) $y = -0.77x + 115.46$ (excluding Mn^{2+}-rich/bearing samples) and (*b*) $y = -3.34x + 115.68$ (excluding the data of uedaite-(Ce) obtained by Miyawaki *et al*., 2008). The regression function in Fig. 4*b* becomes $y = -2.71x + 115.54$ ($R^2 = 0.61$) if the uedaite-(Ce) is included. Standard deviations (1σ) are smaller than the symbol size. Note: Sample K5-700* was plotted from Bonazzi *et al*. (2009). The following samples were not included: (1) Sample YTT, given as allanite-(Ce) (Hoshino *et al*., 2010), because it should be classified as oxyallanite; (2) allanite-(Pb) (Dollase, 1971) and Pb- and *REE*-rich piemontite (Bermanec *et al*., 1994), because of the presence of Pb at *A*1; (3) khristovite-(Ce) (Pautov *et al*., 1993), because of the discrepancy between its structure and chemical composition as noted by Cenki-Tok *et al*. (2006); (4) allanite-(Nd) (Škoda *et al*., 2012), because of the inconsistencies in the structural refinement.

and allanite-group minerals, substitution of Me^{3+} for Al^{3+} at *M*3 and *M*1 increases the *A*1−O6 distance, and thus δ[(*A*1−O6)−(*A*1−O5)]. This implies that epidote-supergroup minerals rich in Al^{3+} at *M*3 and *M*1 have low δ[(*A*1−O6)–(*A*1−O5)] values (e.g. clinozoisite in Fig. 6).

Nomenclature and relationships to other species

Ferriakasakaite-(La) and ferriandrosite-(La) were named in accordance with the recommended nomenclature of epidote-supergroup minerals (Armbruster *et al*., 2006). The new root name 'akasakaite', $^{A1}Ca^{A2}REE^{3+M1}Al^{M2}Al^{M3}Mn^{2+}(Si_2O_7)(SiO_4)O(OH)$, is for minerals in which Ca and Mn^{2+} are the dominant cations at *A*1 and *M*3, respectively. It has already been proposed that a mineral with the chemical composition of akasakaite should be given a new root name in the allanite group (Armbruster *et al*., 2006). In the species studied here, the dominant cation at *M*1 is not Al^{3+} but Fe^{3+} due to the large Fe^{3+} content in the ore sample. Thus, 'ferri' is added as a prefix to the root name 'akasakaite'. A suffix 'La' implying the dominant La at *A*2 is also added. Thus, the name of the new mineral is ferriakasakaite-(La).

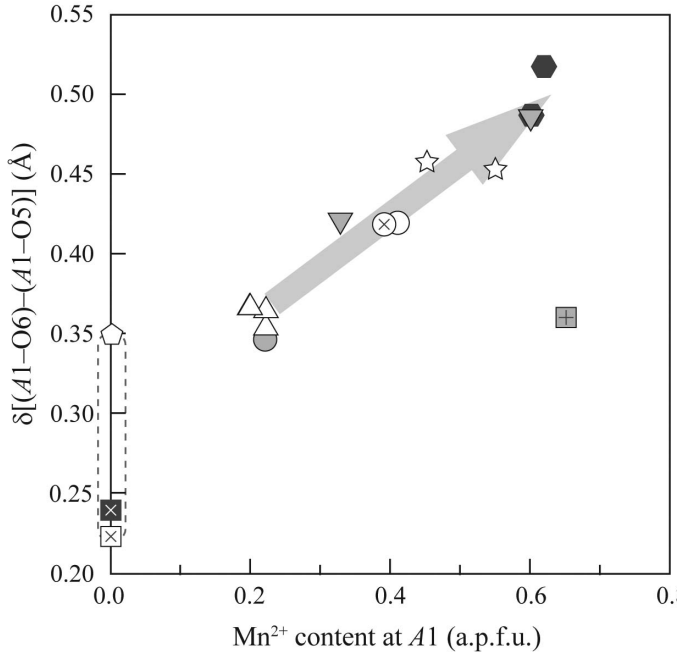

FIG. 6. The variation of δ[(A1−O5)−(A1−O6)] (Å) as a function of Mn^{2+} content at the A1 site. The symbols are same as those in Fig. 5. The dashed line represents the variability range of δ[(A1−O5)−(A1−O6)] derived from Ca-dominant clinozoisite-group minerals (Franz and Liebscher, 2004) and Mn^{2+}-free allanite-group minerals (Dollase, 1971; Bonazzi and Menchetti, 1995; Kartashov *et al*., 2002; Hoshino *et al*., 2005; Orlandi and Pasero, 2006; Rouse and Peacor, 1993; Lavina *et al*., 2006; Hoshino *et al*., 2008). Data for clinozoisite (Dollase, 1968; Comodi and Zanatti, 1997) and ferriallanite-(Ce) (Kartashov *et al*., 2002) are plotted for reference showing its variation.

The proposed new mineral, ferriandrosite-(La), is the ${}^{M1}Fe^{3+}$-analogue of androsite. The root name, androsite, is applied to the species having ${}^{A1}Mn^{2+}{}^{A2}REE^{3+}{}^{M1}Me^{3+}{}^{M2}Al{}^{M3}Mn^{2+}(Si_2O_7)(SiO_4)O(OH)$ with Me^{3+} = Al. Ferriandrosite-(*REE*) has been recommended as the name for possible new members of the androsite subgroup by Armbruster *et al*. (2006; see their table 3). Androsite−akasakaite solid solution is common in most androsite samples, in which Ca often partly dominates at A1 over Mn^{2+} (Cenki-Tok *et al*., 2006; Bonazzi *et al*., 1996).

The new mineral name akasakaite can be applied to the allanite-group mineral with simplified formula Ca*REE*$Fe^{3+}AlMn^{2+}(Si_2O_7)(SiO_4)O(OH)$ described from Kesebol, Västra Götaland, Sweden, by Bonazzi *et al*. (2009). In this mineral, Ce is the dominant lanthanide and it should be named 'ferriakasakaite-(Ce)'. This mineral is strongly metamict. However, the crystal structure could be reconstructed by heat treatment (~800ºC in air and 600/700ºC under N_2), and its structural properties (Bonazzi *et al*., 2009) are similar to those of ferriakasakaite-(La) reported in this study.

Recently, åskagenite-(Nd), $Mn^{2+}NdAlAlFe^{3+}(Si_2O_7)(SiO_4)O_2$, was discovered in a pegmatite body at Åskagen quarry, Sweden (Chukanov *et al*., 2010). It is rich in Mn^{2+} and Fe^{3+} (7.98 wt.% MnO, 7.75 wt.% FeO and 9.16 wt.% Fe_2O_3), and its composition is similar to the species in this study. However, åskagenite-(Nd) is an OH-free epidote-supergroup mineral containing the oxy-allanite component proposed by Hoshino *et al*. (2009, 2010). Thus, its ionic substitution scheme, ${}^{M3}Me^{3+}$ + ${}^{O10}O^{2-}$, is different from that in akasakaite and androsite, ${}^{M3}Me^{2+}$ + ${}^{O10}OH^{-}$.

Acknowledgements

The authors thank Edward Grew (Associate Editor), Paola Bonazzi, Peter Leverett, Peter Williams, Masahide Akasaka and Thomas Armbruster for their constructive comments on

this manuscript. M. Akasaka is thanked for permission to use the Bruker SMART APEXII at Shimane University. One of the authors (M.N.) is supported by a Grant-in-Aid for Young Scientists (B) (No. 25800296) from the Japan Society for the Promotion of Science.

References

Anastasiou, P. and Langer, K. (1977) Synthesis and physical properties of piemontite $Ca_2Al_{3-p}Mn_p^{3+}$ (Si_2O_7/SiO_4/O/OH). *Contributions to Mineralogy and Petrology*, **60**, 225–245.

Armbruster, T., Bonazzi, P., Akasaka, M., Bermanec, V., Chopin, C., Heuss-Assbischler, S., Liebscher, A., Menchetti, S., Pan, Y. and Pasero, M. (2006) Recommended nomenclature of epidote-group minerals. *European Journal of Mineralogy*, **18**, 551–567.

Baur, H. (1974) The geometry of polyhedral distortions. Predictive relationships for the phosphate group. *Acta Crystallographica*, **B30**, 1195–1215.

Bermanec, V., Armbruster, T., Oberhänsli, R. and Zebec, V. (1994) Crystal chemistry of Pb- and *REE*-rich piemontite from Nezilovo, Macedonia. *Schweizerische Mineralogische und Petrographische Mitteilungen*, **74**, 321–328.

Bonazzi, P. and Menchetti, S. (1995) Monoclinic members of the epidote group: effects of the Al ↔ Fe^{3+} ↔ Fe^{2+} substitution and of the entry of REE^{3+}. *Mineralogy and Petrology*, **53**, 133–153.

Bonazzi, P. and Menchetti, S. (2004) Manganese in monoclinic members of the epidote group: piemontite and related minerals. Pp. 495–552 in: *Epidotes* (G. Ferraris and S. Merlino, editors). Reviews in Mineralogy & Geochemistry, **56**. Mineralogical Society of America and the Geochemical Society. Chantilly, Virginia, USA.

Bonazzi, P., Menchetti, S. and Palenzona, A. (1990) Strontiopiemontite, a new member of the epidote group from Val Graveglia, Liguria, Italy. *European Journal of Mineralogy*, **2**, 519–523.

Bonazzi, P., Garbarino, C. and Menchetti, S. (1992) Crystal chemistry of piemontites: *REE*-bearing piemontite from Monte Brugiana, Alpi Apuane, Italy. *European Journal of Mineralogy*, **4**, 23–33.

Bonazzi, P., Menchetti, S. and Reinecke, T. (1996) Solid solution between piemontite and androsite-(La), a new mineral of the epidote group from Andros Island, Greece. *American Mineralogist*, **81**, 735–742.

Bonazzi, P., Holtstam, D., Bindi, L., Nysten, P. and Capitan, G. (2009) Multi-analytical approach to solve the puzzle of an allanite-subgroup mineral from Kesebol, Västra Götaland, Sweden. *American Mineralogist*, **94**, 121–134.

Bruker (1999) *SMART and SAINT-Plus. Versions 6.01*. Bruker AXS Inc., Madison, Wisconsin, USA.

Cenki-Tok, B., Ragu, A., Armbruster, T., Chopin, S. and Medenbach, O. (2006) New Mn- and rare-earth-rich epidote-group minerals in metacherts: manganiandrosite-(Ce) and vanadoandrosite-(Ce). *European Journal of Mineralogy*, **18**, 569–582.

Chukanov, N.V., Göttlicher, J., Möckel, S., Sofer, Z., Van, K.V. and Belakovskiy, D.I.. (2010) Åskagenite-(Nd), $Mn^{2+}NdAl_2Fe^{3+}(Si_2O_7)(SiO_4)O_2$, a new mineral of the epidote supergroup. *New Data on Minerals*, **45**, 17–22.

Comodi, P. and Zanazzi, P. F. (1997) The pressure behavior of clinozoisite and zoisite: An X-ray diffraction study. *American Mineralogist*, **82**, 61–68.

Dollase, W.A. (1968) Refinement and comparison of the structures of zoisite and clinozoisite. *American Mineralogist*, **53**, 1882–1898.

Dollase, W.A. (1971) Refinement of the crystal structures of epidote, allanite and hancockite. *American Mineralogist*, **56**, 447–464.

Franks, F. (Editor) (1973) *Water: A Comprehensive Treatise*, **Vol. 2**. Plenum, New York.

Franz, G. and Liebscher, A. (2004) Physical and chemical properties of the epidote minerals – an introduction. Pp. 1–82 in: *Epidotes* (G. Ferraris and S. Merlino, editors). Reviews in Mineralogy & Geochemistry, **56**. Mineralogical Society of America and the Geochemical Society. Chantilly, Virginia, USA.

Fujinaga, K., Nozaki, T., Nishiuchi, T., Kuwahara, K. and Kato, Y. (2006) Geochemistry and origin of Ananai stratiform manganese deposit in the Northern Chichibu Belt, Central Shikoku, Japan. *Resource Geology*, **56**, 399–414.

Fujinaga, K., Nozaki, T., Nakayama, K. and Kato, Y. (2011) Rare earth resource potential of the Aki strata-bound Fe-Mn deposit in the Northern Shimanto Belt, central Shikoku, Japan. *Shigen-Chishitsu*, **61**, 1–11.

Gieré, R. and Sorensen, S.S. (2004) Allanite and other *REE*-rich epidote-group minerals. Pp. 431–493 in: *Epidotes* (G. Ferraris and S. Merlino, editors). Reviews in Mineralogy & Geochemistry, **56**. Mineralogical Society of America and the Geochemical Society. Chantilly, Virginia, USA.

Giuli, G., Bonazzi, P. and Menchetti, S. (1999) Al-Fe disorder in synthetic epidotes: a single-crystal X-ray diffraction study. *American Mineralogist*, **84**, 933–936.

Hoshino, M., Kimata, M., Nishida, N., Kyono, A., Shimizu, M. and Takizawa, S. (2005) The chemistry of allanite from the Daibosatsu Pass, Yamanashi, Japan. *Mineralogical Magazine*, **69**, 403–423.

Hoshino, M., Kimata, M., Nishida, N., Kyono, A. and

Shimizu, M. (2008) Crystal chemical significance of chemical zoning in dissakisite-(Ce). *Physics and Chemistry of Minerals*, **35**, 59−70.

Hoshino, M., Kimata, M., Chesner, C.A., Nishida, N. and Shimizu, M. (2009) First report of natural oxyallanite: oxidation and dehydration during welding of volcanic tuff. *Abstracts of the Annual Meeting of Japan Association of Mineralogical Sciences 2009*, p. 72.

Hoshino, M., Kimata, M., Chesner, C.A., Nishida, N., Shimizu, M. and Akasaka, T. (2010) Crystal chemistry of volcanic allanites indicative of naturally induced oxidation-dehydration. *Mineralogy and Petrology*, **99**, 133−141.

Ito, T., Morimoto, N. and Sadanaga, R. (1954) On the structure of epidote. *Acta Crystallographica*, **7**, 53−59.

Izumi, F. and Momma, K. (2007) Three-dimensional visualization in powder diffraction. *Solid State Phenomena*, **130**, 15−20.

Kartashov, P.M., Ferraris, G., Ivaldi, G., Sokolova, E. and McCammon, C.A. (2002) Ferriallanite-(Ce), $CaCeFe^{3+}AlFe^{2+}(SiO_4)(Si_2O_7)O(OH)$, a new member of the epidote group: description, X-ray and Mössbauer study. *The Canadian Mineralogist*, **40**, 1641−1648.

Kato, Y., Fujinaga, K., Nozaki, T., Osawa, H., Nakamura, K. and Ono, R. (2005) Rare earth, major and trace elements in the Kunimiyama ferromanganese deposit in the Northern Chichibu belt, Central Shikoku, Japan. *Resource Geology*, **55**, 291−299.

Katoh, K. (1995) The Chichibu Belt of Watarai-cho and Omiya-cho, Mie Prefecture in the eastern Kii Peninsula, Mie Prefecture, Japan. *Journal of the Geological Society of Japan*, **101**, 211−227.

Langer, K., Tillmanns, E., Kersten, M., Almen, H. and Arni, R.K. (2002) The crystal chemistry of Mn^{3+} in the clino- and orthozoisite structure types, $Ca_2M_3^{3+}[OH/O/SiO_4/Si_2O_7]$: a structural and spectroscopic study of some natural piemontites and "thulites" and their synthetic equivalents. *Zeitschrift für Kristallographie*, **217**, 563−580.

Lavina, B., Carbonin, S., Russo, U. and Tumiati, S. (2006) The crystal structure of dissakisite-(La) and structural variations after annealing of radiation damage. *American Mineralogist*, **91**, 104−110.

Mills, S.J., Hatert, F., Nickel, E.H. and Ferraris, G. (2009) The standardisation of mineral group hierarchies: application to recent nomenclature proposals. *European Journal of Mineralogy*, **21**, 1073−1080.

Miyawaki, R., Tokoyama, K., Matsubara, S., Tsutsumi, Y. and Goto, A. (2008) Uedaite-(Ce), a new member of the epidote group with Mn at the A site, from Shodoshima, Kagawa Prefecture, Japan. *European Journal of Mineralogy*, **20**, 261−269.

Momma, K. and Izumi, F. (2011) VESTA3 for three-dimensional visualization of crystal, volumetric and morphology data. *Journal of Applied Crystallography*, **44**, 1257−1276.

Moriyama, T., Miyawaki, R., Yokoyama, K., Matsubara, S., Hirano, H., Murakami, H. and Watanabe, Y. (2010) Wakefieldite-(Nd), a new neodymium vanadate mineral in the Arase Stratiform ferromanganese deposit, Kochi Prefecture, Japan. *Resource Geology*, **61**, 101−110.

Nagashima, M. and Akasaka, M. (2004) An X-ray Rietveld study of piemontite on the join $Ca_2Al_3Si_3O_{12}(OH)-Ca_2Mn_3^{3+}Si_3O_{12}(OH)$ formed by hydrothermal synthesis. *American Mineralogist*, **89**, 1119−1129.

Nagashima, M., Geiger, C.A. and Akasaka, M. (2009) A crystal-chemical investigation of clinozoisite synthesized along the join $Ca_2Al_3Si_3O_{12}(OH)$–$Ca_2Al_2CrSi_3O_{12}(OH)$. *American Mineralogist*, **94**, 1351−1360.

Nagashima, M., Armbruster, T., Akasaka, M. and Minakawa, T. (2010) Crystal chemistry of Mn^{2+}-, Sr-rich and *REE*-bearing piemontite from the Kamisugai mine in the Sambagawa metamorphic belt, Shikoku, Japan. *Journal of Mineralogical and Petrological Sciences*, **105**, 142−150.

Nagashima, M., Imaoka, T. and Nakashima, K. (2011) Crystal chemistry of Ti-rich ferriallanite-(Ce) from Cape Ashizuri, Shikoku Island, Japan. *American Mineralogist*, **96**, 1870−1877.

Nagashima, M., Nishio-Hamane, D., Tomita, N., Minakawa, T. and Inaba, S. (2013) Vanadoallanite-(La): a new epidote-supergroup mineral from Ise, Mie Prefecture, Japan. *Mineralogical Magazine*, **77**, 2739−2752.

Nishio-Hamane, D., Tomita, N., Minakawa, T. and Inaba, S. (2013) Iseite, $Mn_2Mo_3O_8$, a new mineral from Ise, Mie Prefecture, Japan. *Journal of Mineralogical and Petrological Sciences*, **108**, 37−41.

Orlandi, P. and Pasero, M. (2006) Allanite-(La) from Buca della Vena mine, Apuan Alps, Italy, an epidote-group mineral. *The Canadian Mineralogist*, **44**, 63−68.

Pautov, L.A., Khorov, P.V., Ignatenko, K.I., Sokolova, E.V. and Nadezhina, T.N. (1993) Khristovite-(Ce)–(Ca, *REE*)*REE*(Mg, Fe)$AlMnSi_3O_{11}(OH)(F,O)$: a new mineral in the epidote group. *Proceedings of the Russian Mineralogical Society*, **122**, 103−111 .

Peacor, D.R. and Dunn, P.J. (1988) Dollaseite-(Ce) (magnesium orthite redefined): structure refinement and implications from F + M^{2+} substitutions in epidote-group minerals. *American Mineralogist*, **73**, 838−842.

Robinson, K., Gibbs, G.V. and Ribbe, P.H. (1971) Quadratic elongation: a quantitative measure of

distortion in coordination polyhedra. *Science*, **172**, 567–570.

Rouse, R. and Peacor, D. (1993) The crystal structure of dissakisite-(Ce), the Mg analogue of allanite-(Ce). *The Canadian Mineralogist*, **31**, 153–157.

Sheldrick, G.M. (1996) *SADABS*. University of Göttingen, Germany.

Sheldrick, G.M. (2008) A short history of SHELX. *Acta Crystallographica*, **A64**, 112–122.

Škoda, R., Cempírek, J., Filip, J., Novák, M., Veselovský, F. and Čtvrtlík, R. (2012) Allanite-(Nd), $CaNdAl_2Fe^{2+}(SiO_4)(Si_2O_7)O(OH)$, a new mineral from Åskagen, Sweden. *American Mineralogist*, **97**, 983–988.